

EFFICACY OF DATA-FREE METRICS: ROBUST AND CRITICAL EVIDENCE FROM ROBUST AND CRITICAL LAYERS

006 **Anonymous authors**

007 Paper under double-blind review

ABSTRACT

013 Data-free methods for analysing and understanding the layers of neural networks
 014 have offered many metrics for quantifying notions of “strong” versus “weak”
 015 layers, with the promise of increased interpretability. We examine the robustness
 016 and predictive power of data-free metrics under randomised control conditions
 017 across a wide range of models, datasets and architectures. Contrary to some of the
 018 literature, we find strong evidence *against* the efficacy of data-free methods. We
 019 show that they are not reparametrisation-invariant even for *robust* layers, that is
 020 to say layers that can be reparametrised by re-initialisation or re-randomisation
 021 without affecting the accuracy of the model. Moreover, we also show that data-
 022 free metrics cannot be used for the arguably simpler tasks of (i) distinguishing
 023 between robust layers and critical layers, i.e. layers that cannot be reparametrised
 024 without significantly degrading the accuracy of the model, or (ii) predicting if there
 025 will be a performance difference between re-initialisation and re-randomisation.
 026 Thus, we argue that to understand neural networks, and in particular the difference
 027 between ‘strong’ versus “weak” layers, we must adopt mechanistic and functional
 028 approaches, contrary to the traditional Random Matrix Theory perspective.

1 INTRODUCTION

031 Understanding and interpreting deep learning models is a critical area of research, especially as the
 032 prevalence of these models increases in real-world applications. The holy grail of neural network
 033 interpretability lies in identifying computationally cheap metrics that can provide insights into the
 034 effectiveness of neural networks and their components. Data-free methods typify this endeavour
 035 by analysing the properties of the neural network parameters without regard for the data. A key
 036 example of data-free methods is Martin & Mahoney (2021), which claims to be able to predict the
 037 performance of a neural network without the requirement of test data through the use of Random
 038 Matrix Theory to analyse the layer weight matrices. In contrast, data-dependent layer analysis via
 039 mechanistic interpretability or functional analysis attempts to quantify how inputs interact at specific
 040 layers and use comparative analysis to understand the interaction between model parameters and data
 041 (Olah et al., 2020; Klabunde et al., 2025; Nanda et al., 2023).

042 Zhang et al. (2022) identified an interesting and unexpected phenomenon in neural network layers:
 043 some layers within a network are robust, while others are critical. A critical layer is a layer that cannot
 044 be re-initialised or re-randomised without dramatically affecting the performance of the network.
 045 In contrast, a robust layer can be either re-initialised or re-randomised without any noticeable
 046 effect on performance. Re-initialisation sets the layer back to its initial parameters before training,
 047 whilst re-randomisation sets the parameters of the layer to random values by re-sampling from the
 048 same distribution used for initialisation. It was observed that in some cases, re-initialisation and re-
 049 randomisation can result in significant performance differences for a given layer, with re-initialisation
 050 maintaining performance but re-randomisation significantly degrading it (Zhang et al., 2022). In other
 051 cases, re-initialisation and re-randomisation of a layer lead to a negligible difference in performance.

052 We follow in the footsteps of Dinh et al. (2017) which studied another type of metrics, namely
 053 metrics for minima flatness and how they (fail to) relate to generalisation. In particular, the authors
 make the following point: “*Since we are interested in finding a prediction function in a given family*

054 *of functions, no reparametrisation of this family should influence generalisation of any of these*
 055 *functions*”. In the same spirit, the robustness phenomenon suggests that certain reparametrisations
 056 of this family – re-initialisations and re-randomisations of robust layers – should not influence the
 057 functional behaviour of any of these functions (as quantified by accuracy). We believe that this
 058 provides a strong basis for asking:

- 060 • Are data-free metrics reparameterisation-invariant, particularly under re-initialisations or
 061 re-randomisations of robust layers?
- 062 • Can data-free metrics distinguish robust layers from critical layers?
- 063 • Can data-free metrics predict performance difference between re-initialisation and re-
 064 randomisation of a layer?

066 In contrast to Dinh et al. (2017), our approach is purely empirical and our experiments show that
 067 across data modalities, architectures and datasets:

- 068 • Data-free metrics are not invariant under reparametrisation, even when we restrict our
 069 attention to re-initialisations and re-randomisations of robust layers,
- 070 • Current data-free analyses have no predictive capacity to identify robust and critical layers
 071 in small scale experiments, nor to predict performance difference between re-initialisation
 072 and re-randomisation,
- 073 • For Large Language Models (LLMs) and ImageNet vision models norm-based metrics have
 074 no predictive capacity over the change in performance under re-randomisation.

076 We hope that our work can push the field forward in two core ways.

- 078 • To provide a strong test ground for the development of data-free metrics that are able to
 079 disambiguate between robust and critical layers. Similar to how the work of Dinh et al.
 080 (2017) led to the development of sharpness metrics Relative Flatness (Petzka et al., 2021)
 081 and Fisher Rao norm (Liang et al., 2019) that are reparameterisation invariant and now
 082 considered state of the art sharpness metrics.
- 083 • Offering concrete evidence for the prioritisation of data-based metrics, until the appropriate
 084 data-free metrics are discovered, such as those that we examine in the paper to improve
 085 efforts in interpretability and compression.

087 2 BACKGROUND

090 Data-free methods of interpretability aim to understand the inner workings of neural networks by
 091 studying the properties of the network parameters. Data-free approaches often focus on the matrix
 092 norm properties of layer weight matrices to understand learning or improve the performance of neural
 093 networks (Yunis et al., 2024; Martin et al., 2021; Sanyal et al., 2020; Feng et al., 2022; Salimans
 094 & Kingma, 2016; Bartlett et al., 2017) (Wei et al., 2022; Qing et al., 2024; Thamm et al., 2024; He
 095 et al., 2025). However, Zhang et al. (2022) showed in their work that matrix norms, such as the
 096 Frobenius norm, are too coarse to understand the generalisation properties of neural networks. Martin
 097 & Mahoney (2021) use Random Matrix Theory (RMT) to analyse the weight matrices (excluding
 098 biases) of neural network layers through training to create a theory of heavy-tailed self-regularisation.
 099 With this theory, they construct a set of predominately power-norm metrics related to generalisation
 100 that is applied after training to assess layer performance: alpha (α), alpha-weighted ($\hat{\alpha}$), log alpha
 101 norm, and MP soft rank Martin & Mahoney (2021). In this work, they identified a value of α between
 102 2 and 6 as a property of a good, well-trained layer, whereas $\alpha > 6$ indicates that a layer is underfitted
 103 and $\alpha < 2$ indicates that it is overfitted. Martin et al., Martin et al. (2021) showed a correlation
 104 between these metrics and the generalisation performance of pre-trained models in language and
 computer vision tasks.

105 The theory of heavy-tailed self-regularisation (Martin & Mahoney, 2021) has been used to provide
 106 justification for layer-wise pruning ratios in large language models (Lu et al., 2024), additionally it has
 107 been used to explain and understand stages of the grokking phenomenon (Power et al., 2022) namely,
 pre-grokking, grokking and anti-grokking (Prakash & Martin, 2025). The promise of understanding

108 both redundancy in neural networks and transitions from memorisation to generalisation means that
 109 RMT promises a lot with respect to improving the interpretability of deep neural networks, a topic of
 110 great importance given their increasing adoption across a range of different data domains.

111 Since Zhang et al. (2022) established that norm-based methods are ineffective, our work will focus
 112 on alpha, alpha-weighted, log alpha norm, MP Soft Rank and Generalized von-Neumann Matrix
 113 Entropy (Martin & Mahoney, 2021) as well as Frobenius Norm, Spectral Norm and Stable Rank
 114 (Rudelson & Vershynin, 2007) within the critical and robust layer phenomenon to establish whether
 115 these metrics are invariant under re-initialisation and re-randomisation of robust layers and if they
 116 can disambiguate between (i) robust and critical layers, and (ii) the performance difference between
 117 re-initialisation and re-randomisation of a layer.

118

119

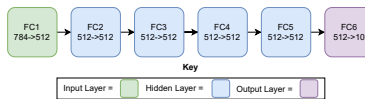
120 3 EXPERIMENTAL SETUP

121

122 Zhang et al. (2022), showed the robust and critical layer phenomenon across a range of trained
 123 architectures, MLPs, VGGs (Simonyan & Zisserman, 2015), ResNets (He et al., 2016), Transformers
 124 (Vaswani et al., 2017), Vision Transformers (Dosovitskiy et al., 2021a), MLPMixers (Tolstikhin et al.,
 125 2021) across datasets MNIST (LeCun et al., 1998), CIFAR10 (Krizhevsky & Hinton, 2009), ImageNet
 126 (Deng et al., 2009) and LM1B (Chelba et al., 2014). We first choose the simplest model (ReLU FCN
 127 5x512), Figure 1, and dataset (MNIST (LeCun et al., 1998)) identified by Zhang et al. (2022) that
 128 demonstrates this phenomenon to systematically explore the behaviour of data-free metrics under
 129 layer re-initialisations and re-randomisations of a large number of trained models.

130

131



132

133

134 Figure 1: ReLU FCN 5x512 Model Architecture.

135

136

137 An added benefit of the ReLU FCN 5x512 model is that it also offers a clear performance contrast
 138 between re-initialisation and re-randomisation. Zhang et al. (2022) showed that residual blocks are
 139 robust to re-randomisation and attributed this to the residual layer potentially playing a lesser role in
 140 the network and thus having smaller activations than the skip connection. To analyse how effective
 141 the data-free metrics are at disambiguating between re-initialisation and re-randomisation, we analyse
 142 the correlation between data-free metrics and test accuracy using the Spearman correlation coefficient
 143 ρ , the root mean square error (RMSE) of the linear regression and Kendall's tau measure ($K-\tau$).
 144 Where ρ and $K-\tau$ score of -1 indicates a very strong negative correlation, 0 indicates no correlation,
 145 and 1 indicates a very strong positive correlation. We use RMSE and Kendall's Tau measure for this
 146 study as they are two of the correlation metrics used in Martin et al. (2021) to highlight the predictive
 147 capacity of the data-free metrics.

148

149

150 We trained 100 ReLU FCN 5x512 models, creating 100 initialisations and 100 trained models, to
 151 obtain a representative sample of possible initialisations and trained models. The model weights and
 152 biases are initialised and re-randomised from the same distribution $\mathcal{U}(-\sqrt{k}, \sqrt{k})$ where k is $\frac{1}{\text{in_features}}$,
 153 e.g. FC1 has $k = \frac{1}{784}$. We record the data-free metric properties of these trained models' layers when
 154 they undergo re-initialisation and re-randomisation and observe whether these metrics:

155

156

157

- (a) are invariant, particularly for robust layers,
- (b) can distinguish critical and robust layers,
- (c) can predict the performance difference between re-initialisation and re-randomisation.

158

159

160 This exploration also demonstrates the overall predictive capacity of data-free metrics after training.

161

Data-Free Metrics. Power Norm based data-free methods analyse a layer weight matrix, W ,
 162 excluding the bias. A variety of data-free metrics have been developed in the literature to quantify the
 163 importance of a layer, we focus on the following metric (Martin & Mahoney, 2021):

162
163
164

- **Alpha** (α): The fitted power law exponent, α , for the empirical spectral density of the correlation matrix $X = W^T W$, such that $p_{emp}(\lambda) \sim \lambda^{-\alpha}$, with λ the eigenvalues of X .

165 In section 4.2 we additionally explore the following metrics:

166
167
168

- **Alpha Weighted** ($\hat{\alpha}$): $\alpha \log(\lambda_{max})$, where λ_{max} is the max eigenvalue from X Martin & Mahoney (2021).
- **Log Alpha Norm**: $\log(\|X\|_\alpha^\alpha)$, where $\|X\|_\alpha^\alpha = \sum_i^M \lambda_i^\alpha$, where M is the rank of W Martin & Mahoney (2021).
- **MP Soft Rank**: is the ratio between the bulk edge of the $p_{emp}(\lambda)$, λ^+ , and the max eigenvalue, λ_{max} , $\frac{\lambda^+}{\lambda_{max}}$ Martin & Mahoney (2021).
- **Spectral Norm**: The max singular value of W denoted as $\|W\|_\infty$.
- **Stable Rank**: The ratio of the squared Frobenius Norm and the squared Spectral Norm, denoted as $\frac{\|W\|_F^2}{\|W\|_2^2}$ Rudelson & Vershynin (2007).
- **Generalized von-Neumann Matrix Entropy**: $\frac{-1}{\log(M)} \sum_i p_i \log p_i$, where M is the rank of matrix W and p_i is $\frac{\sigma_i^2}{\sum_i (\sigma_i^2)}$ where σ is the singular values of W Martin & Mahoney (2021).

182 The metrics are collected using the weightwatcher¹ tool.

183
184 We extend our analysis of questions (a) and (b) to large-scale pre-trained computer vision models
185 (ResNet34² (Wightman et al., 2021; Wightman, 2019; He et al., 2016) and ViT³ (Steiner et al., 2021;
186 Dosovitskiy et al., 2021b; Wightman, 2019), both trained on ImageNet(Russakovsky et al., 2015))
187 and pre-trained large language models (GPT2⁴ and GPT2-Large⁵ (Radford et al., 2019) evaluated on
188 WikiText103 (Merity et al., 2016)), in Section 5.

190 4 RESULTS AND DISCUSSION FOR SMALL SCALE REPARAMETRISATIONS

191
192 For clarity and succinctness, we primarily present our results for alpha (α) of Martin & Mahoney
193 (2021) in the body of the paper, however in Section 4.2 we show that these result generalise to
194 additional metrics. In Appendix Section A we present the analysis of the Frobenius Norm.

196 4.1 ANALYSIS OF ALPHA UNDER RE-INITIALISATION AND RE-RANDOMISATION

197
198 Table 1: Alpha (α) of the layers in ReLU FCN 5x512 and test accuracy of the model. Mean and
199 ± 1 SEM (Belia et al., 2005) (Standard Error from the Mean) derived from 100 trained models on
200 MNIST.

201

Metric	Layer						Test Accuracy
	FC1	FC2	FC3	FC4	FC5	FC6	
Alpha (α)	4.82 ± 0.025	4.205 ± 0.039	4.126 ± 0.038	4.135 ± 0.035	4.193 ± 0.034	3.793 ± 0.805	96.822 ± 0.057

205
206 **Quality of training vs alpha.** Data-free metrics such as α aim to identify well-trained layers,
207 with a well-trained layer having a value of α between 2 and 6 Martin & Mahoney (2021). This
208 seems to be borne out by training 100 ReLU FCN 5x512 models to good values of test accuracy,
209 achieving $\alpha \in [2, 6]$ for every layer (see Table 1). Whilst well-trained may imply $\alpha \in [2, 6]$ (but more
210 on this below), a simple experiment shows that the converse does not hold. We plot the empirical
211 distribution of α for a 512x512 fully connected layer in Figure 2 (left), sampled from 10,000 potential

212 ¹<https://weightwatcher.ai>

213 ²https://huggingface.co/timm/resnet34.tv_in1k

214 ³https://huggingface.co/timm/vit_base_patch16_224_augreg_in1k

215 ⁴<https://huggingface.co/openai-community/gpt2>

⁵<https://huggingface.co/openai-community/gpt2-large>

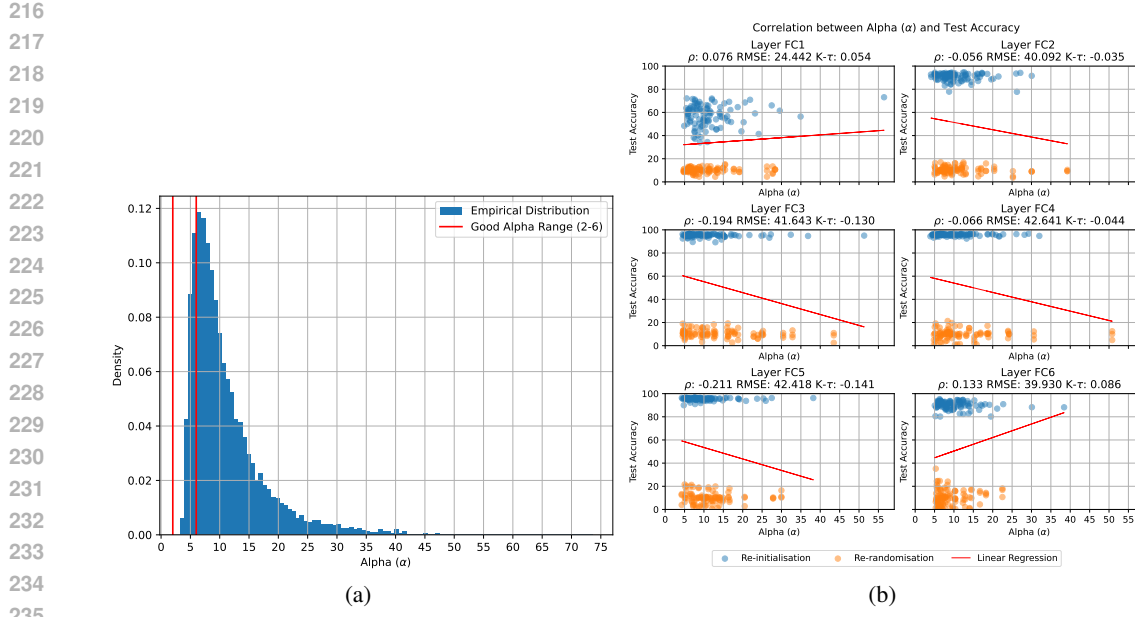


Figure 2: Empirical distribution of α values on a 512x512 fully connected layer, sampled from 10,000 initialisations (**Left**). Layer re-initialisation (**blue**) and re-randomisation (**orange**) test accuracy vs α , ρ is the Spearman correlation coefficient, $RMSE$ is the root mean square error of the linear regression (red line), and $K-\tau$ is the Kendall’s tau measure, all with respect to the relationship between test accuracy and α values (**Right**).

initialisations. The resulting distribution shows that an initialised, *untrained* layer of this network, can fall, with a small but non-negligable probability, within the optimal α value range of 2 and 6.

Next, we perform independent re-initialisations (**blue** in Figure 2) and re-randomisations (**orange**) of each layer for 100 trained ReLU FCN 5x512 networks and record the impact on the networks’ test accuracy and alpha values. Figure 2 shows that a non-negligable proportion of networks whose performance is severely degraded by re-randomisation maintain a good value of α around 5. Conversely, many networks maintain good performance after re-initialisations (particularly of layers FC3-FC5) but with α values significantly outside of [2, 6]. Good models can have bad alphas, bad models can have good alphas.

Reparametrisation-invariance of alpha. As is clear from 2, whilst all values of α start in the “good” range [2, 6], reparametrisation in the form of re-initialisation or re-randomisation scatters these values over a very wide range (typically deep into “underfitted” territory), irrespective of the change in accuracy incurred by this reparametrisation. Alpha is not invariant under these reparametrisations, even when accuracy is (i.e. on robust layers).

The robust vs critical phenomenon and alpha Figure 2 shows the stark contrast in how layers respond to re-initialisation and re-randomisation. For example, we only see a large drop in test accuracy when applying re-initialisation to the Layer FC1, re-initialising other layers leaves performance almost unchanged. From this perspective, FC1 is a critical layer whilst FC2-FC6 are robust (to re-initialisation). In this experiment α cannot distinguish between these behaviours, the range of values taken by α shows no noticeable difference between critical and robust layers.

The re-initialisation vs re-randomisation phenomenon and alpha. We observe different results when re-randomisation is applied. We find that re-randomising any layer degrades accuracy to circa random accuracy on the test set, in other words none of the layers are robust to re-randomisation. Surprisingly, this is not reflected in the corresponding α values of these two conditions, as the distribution of α values is relatively similar for each layer and each condition. If α had predictive power we would expect to observe a negative correlation between re-initialisation (corresponding

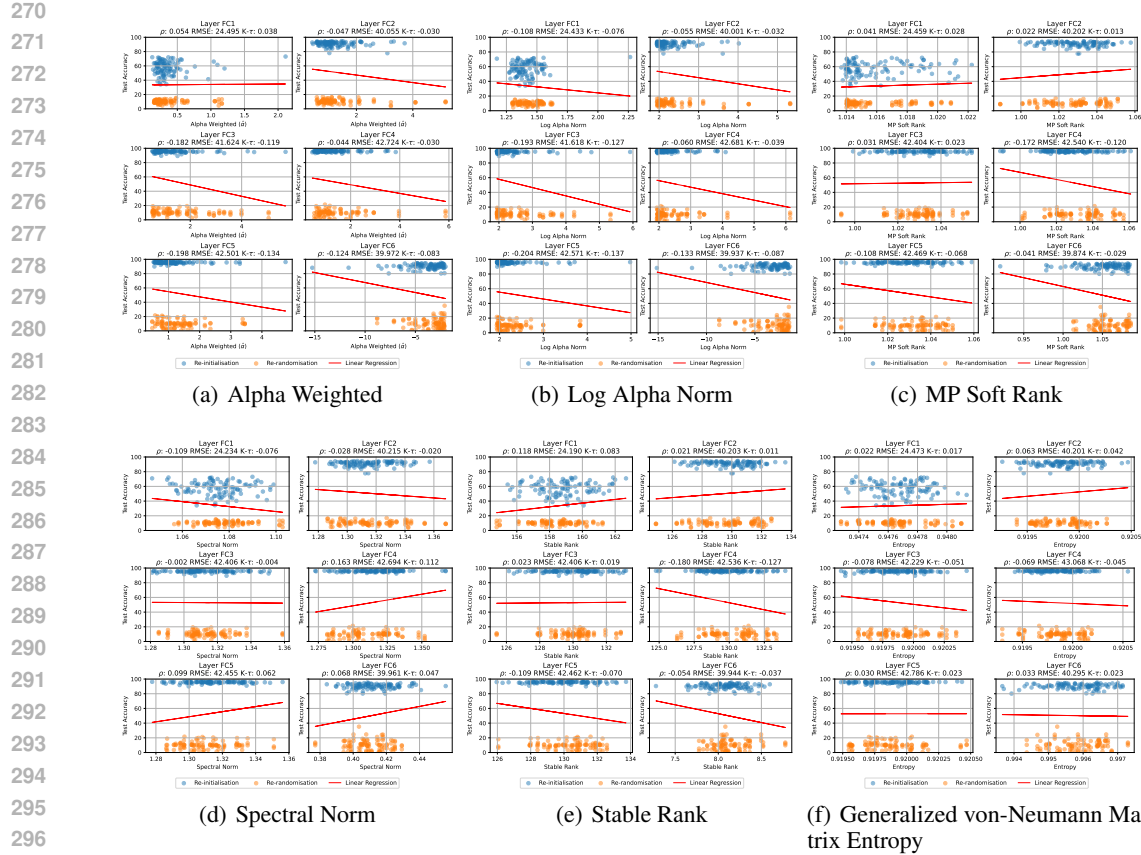


Figure 3: Layer re-initialisation (blue) and re-randomisation (orange) test accuracy vs the respective metric. ρ is the Spearman correlation coefficient, $RSME$ is the root mean square error of the linear regression (red line), and $K-\tau$ is the Kendall’s tau measure, all with respect to the relationship between test accuracy and the metric.

to “good” alphas) to re-randomisation (corresponding to “bad” alphas). However, there is almost no difference between the α values of re-initialisation and re-randomisation, with a mean Spearman correlation coefficient and Kendall’s tau measure across layers of -0.053 and -0.035, respectively. Thus α does not distinguish between these behaviours either. These findings extend to other data-free metrics in Appendix Section A and Section 4.2. Moreover, in Appendix D, we show that α is not causally related to generalisation through two experiments. The first observes how random performance can emerge even when all layers are within the “good” α range ($2 \leq \alpha \leq 6$ and the second shows that training models within and outside of the “good” α range can result in models with equivalent test accuracy.

4.2 GENERALISATION OF REPARAMETRISATION INVARIANCE TO DATA FREE METRICS

We extend our analysis to other data-free metrics that have been defined in literature, we argue that given the lack of predictive power of the α metric in the previous section, it is important to verify across other representative measures that data-free metrics broadly cannot disambiguate between critical and robust layers, between re-initialisation and re-randomisation. When we conduct a similar analysis across six other metrics, Alpha Weighted, Log Alpha Norm, MP Soft Rank, Spectral Norm, Stable Rank and Generalized von-Neumann Matrix Entropy we find, as shown in Figure 3, that we can draw exactly the same conclusion as with α .

324 4.3 COMPARING TO DATA-BASED METRICS
325326 To compare data-free and data-based metrics we explore if two widely used data-based metrics can
327 distinguish the output of a re-initialised layer from that of a re-randomised layer.328 The outputs of the original and modified layers are represented as \mathcal{O}_l and \mathcal{M}_l , respectively. The
329 model layer outputs are collected by passing through the test dataset, \mathcal{D}_{test} . The metrics explored are
330 defined as follows ([Linear CKA \(Kornblith et al., 2019\) is explored in Appendix C](#)):
331332

- **Activation Disagreement:** The mean percentage of times that the neurons from \mathcal{O}_l and \mathcal{M}_l
333 fail to agree to activate on \mathcal{D}_{test} .
- **Jensen–Shannon (JS) Divergence:** The mean weighted average of the Kullback–Leibler
335 (KL) Divergence of the softmax(\mathcal{O}_l on \mathcal{D}_{test}) compared to the softmax(\mathcal{M}_l on \mathcal{D}_{test}) (Lin,
336 1991).

337 When considering the results of the activation disagreement and JS divergence between the original
338 model layer and each model with re-initialised and re-randomised layers in Figure 4, it becomes
339 clear that there is a stark difference in similarity between the re-initialised and re-randomised layers
340 compared to their original layer. The figure demonstrates that the difference between re-initialisation
341 and re-randomisation can be explained by the amount the layer disagrees on activation compared to
342 the original non-modified layer. It is evident that when there is less disagreement (re-initialisation),
343 the model can maintain accuracy, while a lot of disagreement (re-randomisation) leads to a drop
344 in accuracy. This observation is further supported by a mean Spearman correlation coefficient and
345 Kendall’s tau measure across layers of -0.776 and -0.5375, respectively for Activation Disagreement,
346 indicating a negative relationship between activation disagreement and test accuracy.347 We have produced these results to show that there exist metrics that can disambiguate between
348 re-initialisation and re-randomisation behaviours which we believe deserve increased focus over
349 data-free metrics (whether they can distinguish critical from robust is, in this instance, less clear).350 [In Appendix B, we provide an analysis of data-based metrics via the Lottery Ticket Hypothesis \(Franks
351 & Carbin, 2018\), which shows that the ability to disambiguate robust and critical layers is related
352 to considerations of subnetwork pathways, an inherent consideration of the data-based metrics we
353 survey.](#)355 5 RESULTS AND DISCUSSION FOR LARGE SCALE REPARAMETRISATIONS
356358 We further explore how predictive the α metric can be when predicting performance of layers in
359 large scale models that have been trained for high-complexity tasks using the re-randomisation setup.
360 Overall we find, consistent with our small scale experiments, that the α metric has no predictive
361 capacity under this condition, therefore questioning its utility in predicting the performance of layer
362 criticality and “trainedness”. For these results we employ pre-trained open source models, therefore,
363 we do not have access to the starting initialisation and, as a result, we only focus on the case of
364 re-randomisation to test the predictive capacity of the α metric at this scale. We show the relationship
365 reported in this section is consistent with other data-free metrics in this experimental set up in
366 Appendix Sections A.2, A.3, A.4 and A.5.367 5.1 IMAGENET SCALE
368369 We explore the relationship of a layer’s α value with the corresponding performance of the model on
370 ImageNet with pre-trained ResNet34 and ViT models. The respective performance and model details
371 are shown in Table 2; from this table it can be observed that these models are well trained for the task
372 of ImageNet. In line with the Random Matrix Theory perspective, the competitive performance of
373 these models is aligned with a mean α value across layers within the optimal range, representing two
374 well-fitted networks.375 We employ both the pre-trained ResNet34 and ViT as base models for our re-randomisation ex-
376 periment. To conduct this experiment we randomise a layer independently and then record the
377 corresponding test accuracy and α value post re-randomisation. Given that different implicit biases
respond uniquely to re-randomisation we believe that our selection of models is representative for

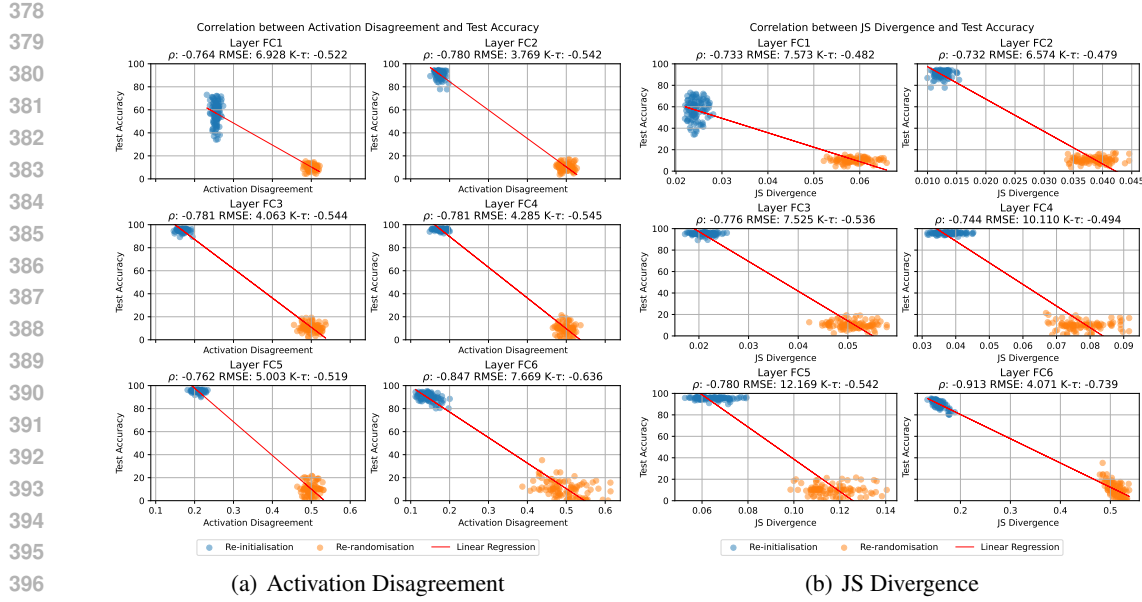


Figure 4: Layer re-initialisation (blue) and re-randomisation (orange) test accuracy vs the respective metric. ρ is the Spearman correlation coefficient, $RMSE$ is the root mean square error of the linear regression (red line), and $K-\tau$ is the Kendall's tau measure, all with respect to the relationship between test accuracy and the metric.

the core architectural differences, allowing a robust analysis of the impacts of re-randomisation and α metrics at scale. We repeat our re-randomisation process 10 times per layer to capture stochastic variation in randomisations. In both ResNet34 and ViT, Figure 5, we find no relationship between α and test accuracy, as found in the small scale experiment. The mean Spearman correlation coefficients are 0.006 and -0.051, and Kendall's tau values are 0.005 and -0.035, respectively.

Table 2: ResNet34 and ViT performance on ImageNet and mean layer Alpha (α) value \pm 1 SEM (Belia et al., 2005) (standard error from the mean).

Model	Number of Parameters	Loss	Accuracy	Mean Layer Alpha Value
ResNet34	21.8M	1.071	73.302	3.380 ± 0.195
ViT	86.6M	0.825	78.852	4.711 ± 0.271

As previously reported in the small-scale experiments, layers in vision models can be re-randomised to α values outside of the desired range but continue to retain accuracy. While in the case of the ResNet34 we see that the model is not so robust to re-randomisation, having a lower accuracy than the baseline, there is a large proportion of layers with optimal α values that result in a model with essentially random accuracy. The ViT is more robust to layer re-randomisation and show the inverse case where many layers are significantly outside of the optimal α range but display a high preservation of the baseline accuracy. As a result, for large scale vision models these results confirm that α is not invariant under reparametrisation by re-randomisation, even on robust layers, and has very limited predictive capacity over post re-randomisation performance.

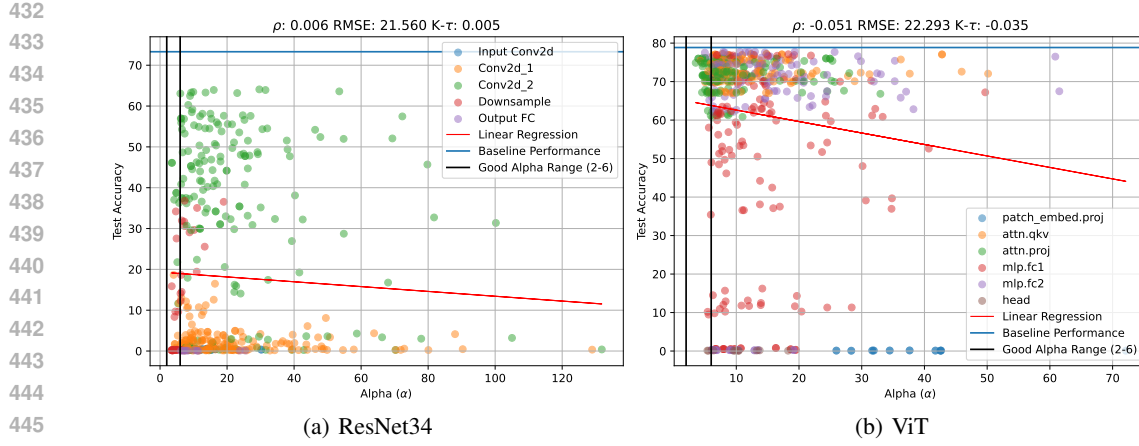


Figure 5: ResNet34 and ViT layer re-randomisation Test Accuracy vs Alpha (α) on ImageNet. ρ is the Spearman correlation coefficient, $RMSE$ is the root mean square error of the linear regression (red line), and $K-\tau$ is the Kendall’s tau measure, all with respect to the relationship between the performance and α values.

5.2 LARGE LANGUAGE MODELS

Given our negative results for the predictive capacity of the α metric in the vision domain under re-randomisation, it is important to verify the generality of our findings under a different modality. Therefore, we have extended the exploration of the relationship of a layers α value and the corresponding performance of the model to language models on WikiText103 with pre-trained GPT2 and GPT2-Large, the respective performance and model details is shown in Table 3. These models represent an increased scale of our experiments as they have hundreds of millions of parameters. Both models have competitive performance with low loss and perplexity on the WikiText-103 datasets and, in-line with Random Matrix Theory have mean layer α values that are within the optimal range.

Table 3: GPT and GPT-Large Test performance on WikiText-103 and mean layer Alpha (α) value \pm 1 SEM (Belia et al., 2005) (standard error from the mean).

Model	Number of Parameters	Loss	Perplexity	Mean Layer Alpha Value
GPT	127M	3.399	29.941	3.865 ± 0.136
GPT-Large	774M	2.967	19.436	4.013 ± 0.091

We use the pre-trained models as the base model and then we randomise a layer and record its α value and the corresponding test perplexity and loss of the model. We do this 10 times for each layer to obtain a representative set of random layers. For both GPT2 and GPT2-Large, Figure 6 we observe that their is no relationship between the performance of the model and a layer’s α value, with a mean Spearman correlation coefficient of 0.028, 0.116 and Kendall’s tau measure of 0.018 and 0.078 for GPT2 and GPT2-Large receptively. We also find that randomising layers in the GPT2 and GPT2-Large model often has a negligible affect on the performance of the model irrespective of the α value associated with the layer. Furthermore, when re-randomising a layer and achieving negligible performance degradation we can observe that the bulk of these layers are far outside the optimal range provided by the α metric. Again, we see that α is not invariant under reparametrisation by re-randomisation, even on robust layers, and has no predictive power over performance.

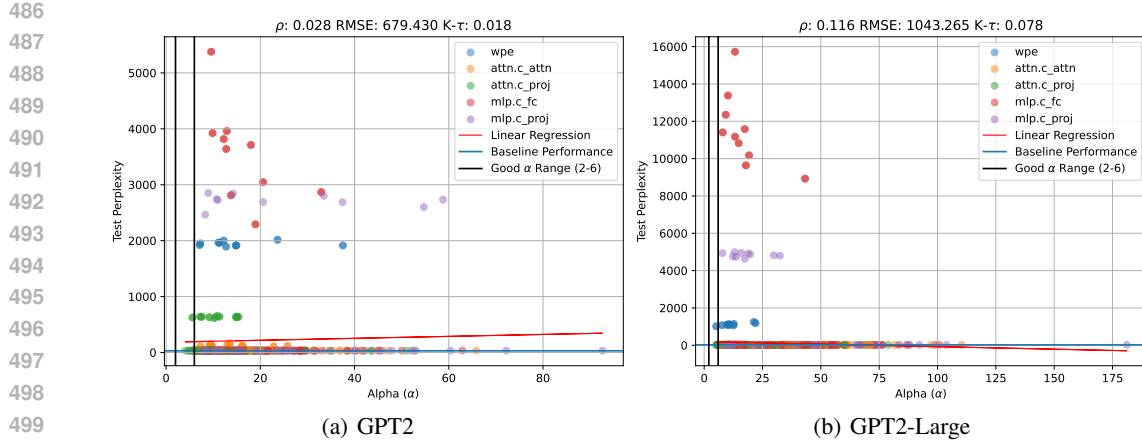


Figure 6: GPT2 and GPT2-Large layer re-randomisation Test Perplexity vs Alpha (α) on WikiText103. ρ is the Spearman correlation coefficient, $RMSE$ is the root mean square error of the linear regression (red line), and $K-\tau$ is the Kendall’s tau measure, all with respect to the relationship between the performance and α values.

6 CONCLUSION

In this work we concretely showed that data-free metrics cannot explain the robust vs critical layer phenomenon, nor the re-initialisation vs re-randomisation phenomenon. Based on experiments covering a wide range of these metrics and a wide range of models, we argue that they have little to no predictive capacity over these important performance-related layer properties. We highlighted how data-free metrics can be described as non-reparameterisation invariant even for robust layers for which accuracy is (to some degree) reparameterisation invariant. Our results scaling from MNIST to ImageNet and Large Language Models confirm the generality of the robustness of our findings. Finally we argue that the correlations of the alpha (and other data-free metrics) fail because they do not capture the nuanced interplay between both the data passed through the model and the weights that process it.

Concretely our recommendations are as follows:

- Avoid the use of data-free that only have spurious relations with model performance and are not a necessary prerequisite of generalisation.
- Ensure that novel data-free metrics are able to meaningfully capture performance differences offered by re-initialisation and re-randomisation.
- In lieu of such data-free metrics, to pursue understanding neural networks with metrics that consider the crucial interplay between weights and data.
- Prioritise data-based approaches for interpretability due to their capability of capturing the meaningful differences between re-initialisation and re-randomisation.

As a consequence, our results advocate for a reappraisal of the way that we approach interpretability of neural networks. Instead of using metrics which lack predictive capacity, we argue that there is a requirement for an in-depth exploration of data-free methods that can suitably disambiguate between the robust and critical layer phenomena. Or rather, a focus on methods that consider more than just weight distributions of models, which we show can be arbitrarily reparametrised without impacting the performance, and instead seek metrics which further understand the more nuanced interplay between weights and data.

REFERENCES

Peter L Bartlett, Dylan J Foster, and Matus J Telgarsky. Spectrally-normalized margin bounds for neural networks. In *Advances in Neural Information Processing Systems*, vol-

540 ume 30, 2017. URL https://papers.nips.cc/paper_files/paper/2017/hash/b22b257ad0519d4500539da3c8bcf4dd-Abstract.html.
541
542
543 Sarah Belia, Fiona Fidler, Jennifer Williams, and Geoff Cumming. Researchers misunderstand
544 confidence intervals and standard error bars. *Psychological methods*, 10(4):389, 2005. URL
545 <https://psycnet.apa.org/record/2005-16136-002>.
546
547 Ciprian Chelba, Tomas Mikolov, Mike Schuster, Qi Ge, Thorsten Brants, Philipp Koehn, and Tony
548 Robinson. One billion word benchmark for measuring progress in statistical language modeling,
549 2014. URL <https://arxiv.org/abs/1312.3005>.
550
551 Jia Deng, Wei Dong, Richard Socher, Li-Jia Li, Kai Li, and Li Fei-Fei. Imagenet: A large-scale
552 hierarchical image database. In *2009 IEEE conference on computer vision and pattern recognition*,
553 pp. 248–255. Ieee, 2009. URL <https://ieeexplore.ieee.org/document/5206848>.
554
555 Laurent Dinh, Razvan Pascanu, Samy Bengio, and Yoshua Bengio. Sharp minima can generalize for
556 deep nets. In *Proceedings of the 34th International Conference on Machine Learning*, volume 70
557 of *Proceedings of Machine Learning Research*, pp. 1019–1028. PMLR, 2017. URL <https://proceedings.mlr.press/v70/dinh17b.html>.
558
559 Alexey Dosovitskiy, Lucas Beyer, Alexander Kolesnikov, Dirk Weissenborn, Xiaohua Zhai, Thomas
560 Unterthiner, Mostafa Dehghani, Matthias Minderer, Georg Heigold, Sylvain Gelly, Jakob Uszkoreit,
561 and Neil Houlsby. An image is worth 16x16 words: Transformers for image recognition at scale. In
562 *International Conference on Learning Representations*, 2021a. URL <https://openreview.net/forum?id=YicbFdNTTy>.
563
564 Alexey Dosovitskiy, Lucas Beyer, Alexander Kolesnikov, Dirk Weissenborn, Xiaohua Zhai, Thomas
565 Unterthiner, Mostafa Dehghani, Matthias Minderer, Georg Heigold, Sylvain Gelly, Jakob Uszkoreit,
566 and Neil Houlsby. An image is worth 16x16 words: Transformers for image recognition at scale.
567 *ICLR*, 2021b.
568
569 Ruili Feng, Kecheng Zheng, Yukun Huang, Deli Zhao, Michael Jordan, and Zheng-
570 Jun Zha. Rank diminishing in deep neural networks. In *Advances in Neu-
571 ral Information Processing Systems*, volume 35, pp. 33054–33065, 2022. URL
572 https://proceedings.neurips.cc/paper_files/paper/2022/hash/d5cd70b708f726737e2ebace18c3f71b-Abstract-Conference.html.
573
574 Jonathan Frankle and Michael Carbin. The lottery ticket hypothesis: Finding sparse, trainable neural
575 networks. *arXiv preprint arXiv:1803.03635*, 2018.
576
577 Di He, Ajay Jaiswal, Songjun Tu, Li Shen, Ganzhao Yuan, Shiwei Liu, and Lu Yin. Alphadecay:
578 Module-wise weight decay for heavy-tailed balancing in llms. *arXiv preprint arXiv:2506.14562*,
579 2025.
580
581 Kaiming He, Xiangyu Zhang, Shaoqing Ren, and Jian Sun. Deep residual learning for image recogni-
582 tion. In *Proceedings of the IEEE Conference on Computer Vision and Pattern Recognition (CVPR)*,
583 June 2016. URL https://www.cv-foundation.org/openaccess/content_cvpr_2016/html/He_Deep_Residual_Learning_CVPR_2016_paper.html.
584
585 Max Klabunde, Tobias Schumacher, Markus Strohmaier, and Florian Lemmerich. Similarity of neural
586 network models: A survey of functional and representational measures. *ACM Computing Surveys*,
587 57(9):1–52, 2025. URL <https://doi.org/10.1145/3728458>.
588
589 Simon Kornblith, Mohammad Norouzi, Honglak Lee, and Geoffrey Hinton. Similarity of neural
590 network representations revisited. In *Proceedings of the 36th International Conference on Machine
591 Learning*, volume 97, pp. 3519–3529. PMLR, 09–15 Jun 2019.
592
593 Alex Krizhevsky and Geoffrey Hinton. Learning multiple layers of features from tiny images. 2009.
594 URL <http://www.cs.utoronto.ca/~kriz/learning-features-2009-TR.pdf>.
595
596 Yann LeCun, Corinna Cortes, and CJ Burges. Mnist handwritten digit database. *ATT Labs [Online]*.
597 Available: <http://yann.lecun.com/exdb/mnist>, 2, 1998.

594 Tengyuan Liang, Tomaso Poggio, Alexander Rakhlin, and James Stokes. Fisher-rao metric, geometry,
 595 and complexity of neural networks. In *The 22nd international conference on artificial intelligence
 596 and statistics*, pp. 888–896. PMLR, 2019.

597

598 J. Lin. Divergence measures based on the shannon entropy. *IEEE Transactions on Information
 599 Theory*, 37(1):145–151, 1991. doi: 10.1109/18.61115.

600

601 Haiquan Lu, Yefan Zhou, Shiwei Liu, Zhangyang Wang, Michael W. Mahoney, and Yaoqing Yang.
 602 Alphapruning: Using heavy-tailed self regularization theory for improved layer-wise pruning of
 603 large language models. In *The Thirty-eighth Annual Conference on Neural Information Processing
 604 Systems*, 2024. URL <https://openreview.net/forum?id=fHq4x2YXVv>.

605

606 Charles H. Martin and Michael W. Mahoney. Implicit self-regularization in deep neural networks:
 607 Evidence from random matrix theory and implications for learning. *Journal of Machine Learning
 608 Research*, 22(165):1–73, 2021. URL <http://jmlr.org/papers/v22/20-410.html>.

609

610 Charles H Martin, Tongsu Peng, and Michael W Mahoney. Predicting trends in the quality of state-of-
 611 the-art neural networks without access to training or testing data. *Nature Communications*, 12(1):
 612 4122, 2021. URL <https://www.nature.com/articles/s41467-021-24025-8>.

613

614 Stephen Merity, Caiming Xiong, James Bradbury, and Richard Socher. Pointer sentinel mixture
 615 models, 2016.

616

617 Neel Nanda, Lawrence Chan, Tom Lieberum, Jess Smith, and Jacob Steinhardt. Progress measures for
 618 grokking via mechanistic interpretability. In *The Eleventh International Conference on Learning
 619 Representations*, 2023. URL <https://openreview.net/forum?id=9XFSbDPmdW>.

620

621 Chris Olah, Nick Cammarata, Ludwig Schubert, Gabriel Goh, Michael Petrov, and Shan Carter.
 622 Zoom in: An introduction to circuits. *Distill*, 2020. URL <https://distill.pub/2020/circuits-zoom-in>.

623

624 Henning Petzka, Michael Kamp, Linara Adilova, Cristian Sminchisescu, and Mario Boley. Relative
 625 flatness and generalization. *Advances in neural information processing systems*, 34:18420–18432,
 626 2021.

627

628 Alethea Power, Yuri Burda, Harri Edwards, Igor Babuschkin, and Vedant Misra. Grokking: General-
 629 ization beyond overfitting on small algorithmic datasets, 2022. URL <https://arxiv.org/abs/2201.02177>.

630

631 Hari Kishan Prakash and Charles H Martin. Grokking and generalization collapse: Insights from htsr
 632 theory. In *High-dimensional Learning Dynamics* 2025, 2025.

633

634 Peijun Qing, Chongyang Gao, Yefan Zhou, Xingjian Diao, Yaoqing Yang, and Soroush Vosoughi.
 635 Alphalora: Assigning lora experts based on layer training quality. *arXiv preprint arXiv:2410.10054*,
 636 2024.

637

638 Alec Radford, Jeffrey Wu, Rewon Child, David Luan, Dario Amodei, Ilya Sutskever, et al. Language
 639 models are unsupervised multitask learners. *OpenAI blog*, 1(8):9, 2019.

640

641 Mark Rudelson and Roman Vershynin. Sampling from large matrices: An approach through geometric
 642 functional analysis. *J. ACM*, 54(4):21–es, 2007. ISSN 0004-5411. URL <https://doi.org/10.1145/1255443.1255449>.

643

644 Olga Russakovsky, Jia Deng, Hao Su, Jonathan Krause, Sanjeev Satheesh, Sean Ma, Zhiheng Huang,
 645 Andrej Karpathy, Aditya Khosla, Michael Bernstein, Alexander C. Berg, and Li Fei-Fei. ImageNet
 646 Large Scale Visual Recognition Challenge. *International Journal of Computer Vision (IJCV)*, 115
 647 (3):211–252, 2015. doi: 10.1007/s11263-015-0816-y.

648

649 Tim Salimans and Durk P Kingma. Weight normalization: A simple reparameterization to accel-
 650 erate training of deep neural networks. In *Advances in Neural Information Processing Systems*,
 651 volume 29, 2016. URL https://proceedings.neurips.cc/paper_files/paper/2016/hash/ed265bc903a5a097f61d3ec064d96d2e-Abstract.html.

648 Amartya Sanyal, Philip H. Torr, and Puneet K. Dokania. Stable rank normalization for improved gen-
 649 eralization in neural networks and gans. In *International Conference on Learning Representations*,
 650 2020. URL <https://openreview.net/forum?id=H1enKkrFDB>.

651

652 Karen Simonyan and Andrew Zisserman. Very deep convolutional networks for large-scale image
 653 recognition, 2015. URL <https://arxiv.org/abs/1409.1556>.

654 Andreas Steiner, Alexander Kolesnikov, , Xiaohua Zhai, Ross Wightman, Jakob Uszkoreit, and Lucas
 655 Beyer. How to train your vit? data, augmentation, and regularization in vision transformers. *arXiv*
 656 preprint *arXiv:2106.10270*, 2021.

657

658 Matthias Thamm, Max Staats, and Bernd Rosenow. Random matrix theory analysis of neural network
 659 weight matrices. In *High-dimensional Learning Dynamics 2024: The Emergence of Structure and*
 660 *Reasoning*, 2024. URL <https://openreview.net/forum?id=41kpc2Nzwc>.

661 Ilya O Tolstikhin, Neil Houlsby, Alexander Kolesnikov, Lucas Beyer, Xiaohua Zhai,
 662 Thomas Unterthiner, Jessica Yung, Andreas Steiner, Daniel Keysers, Jakob Uszkoreit,
 663 Mario Lucic, and Alexey Dosovitskiy. Mlp-mixer: An all-mlp architecture for vision.
 664 In *Advances in Neural Information Processing Systems*, volume 34, pp. 24261–24272,
 665 2021. URL https://proceedings.neurips.cc/paper_files/paper/2021/file/cba0a4ee5cccd02fda0fe3f9a3e7b89fe-Paper.pdf.

666

667 Ashish Vaswani, Noam Shazeer, Niki Parmar, Jakob Uszkoreit, Llion Jones, Aidan N
 668 Gomez, Łukasz Kaiser, and Illia Polosukhin. Attention is all you need. In
 669 *Advances in Neural Information Processing Systems*, volume 30, 2017. URL
 670 https://proceedings.neurips.cc/paper_files/paper/2017/hash/3f5ee243547dee91fdb053c1c4a845aa-Abstract.html.

671

672 Alexander Wei, Wei Hu, and Jacob Steinhardt. More than a toy: Random matrix models predict how
 673 real-world neural representations generalize. In *International conference on machine learning*, pp.
 674 23549–23588. PMLR, 2022.

675

676 Ross Wightman. Pytorch image models. <https://github.com/huggingface/pytorch-image-models>, 2019.

677

678 Ross Wightman, Hugo Touvron, and Herve Jegou. Resnet strikes back: An improved training
 679 procedure in timm. In *NeurIPS 2021 Workshop on ImageNet: Past, Present, and Future*, 2021.

680

681 David Yunis, Kumar Kshitij Patel, Samuel Wheeler, Pedro Savarese, Gal Vardi, Karen Livescu,
 682 Michael Maire, and Matthew R. Walter. Approaching deep learning through the spectral dynamics
 683 of weights, 2024. URL <https://arxiv.org/abs/2408.11804>.

684

685 Chiyuan Zhang, Samy Bengio, and Yoram Singer. Are all layers created equal? *Journal of Machine*
 686 *Learning Research*, 23(67):1–28, 2022. URL <http://jmlr.org/papers/v23/20-069.html>.

687

688

689 **A FURTHER ANALYSIS ON DATA-FREE METRICS**

690

691 In this section we extend our analysis to the following data free metrics in our existing experimental
 692 setup. W represents the weight matrix of the layer and X is for the empirical spectral density of the
 693 correlation matrix, $X = W^T W$, such that $p_{emp}(\lambda) \sim \lambda^{-\alpha}$, where λ are the eigenvalues of X .

694

- 695 • **Alpha Weighted ($\hat{\alpha}$)**: $\alpha \log(\lambda_{max})$, where λ_{max} is the max eigenvalue from X Martin &
 696 Mahoney (2021).
- 697 • **Log Alpha Norm**: $\log(\|X\|_{\alpha}^{\alpha})$, where $\|X\|_{\alpha}^{\alpha} = \sum_i^M \lambda_i^{\alpha}$, where M is the rank of W Martin
 698 & Mahoney (2021).
- 699 • **MP Soft Rank**: is the ratio between the bulk edge of the $p_{emp}(\lambda)$, λ^+ , and the max
 700 eigenvalue, λ_{max} , $\frac{\lambda^+}{\lambda_{max}}$ Martin & Mahoney (2021).

- **Frobenius Norm:** The sum of the singular values of W denoted as $\|W\|_F$.
- **Spectral Norm:** The max singular value of W denoted as $\|W\|_\infty$.
- **Stable Rank:** The ratio of the squared Frobinues Norm and the squared Spectral Norm, denoted as $\frac{\|W\|_F^2}{\|W\|_2^2}$ Rudelson & Vershynin (2007).
- **Generalized von-Neumann Matrix Entropy:** $\frac{-1}{\log(M)} \sum_i p_i \log p_i$, where M is the rank of matrix W and p_i is $\frac{\sigma_i^2}{\sum_i (\sigma_i^2)}$ where σ is the singular values of W Martin & Mahoney (2021).

Each metric can be found below with the appropriate subsection that corresponds to our analysis of these data-free metrics.

The correlation between the Frobenius Norm and the associated test accuracy when layers undergo re-initialisation (blue) or re-randomisation is shown in Figure 7. The Frobenius Norm observes approximately zero correlation between the metric values and the test accuracy, highlighting the same findings as in the body of the paper.

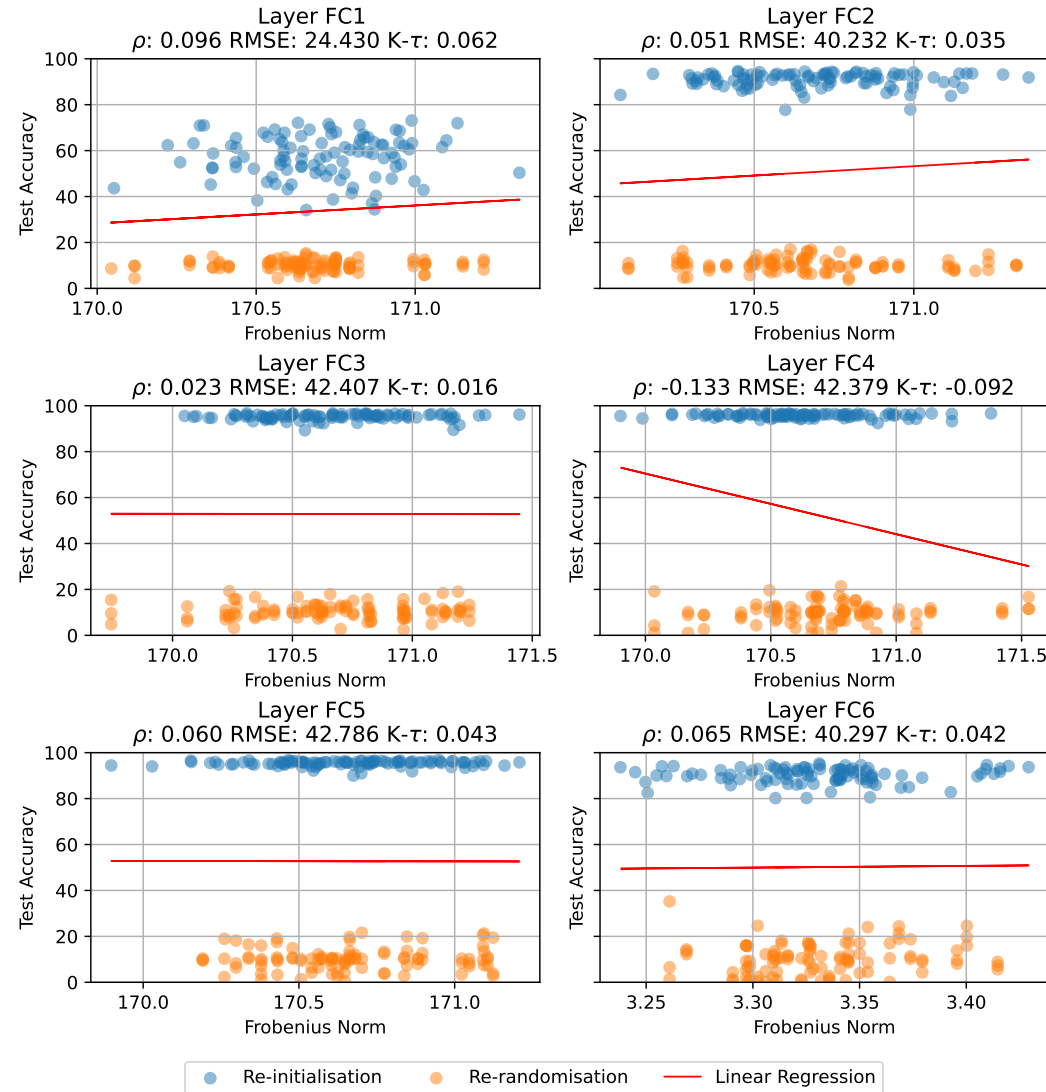
756
757

A.1 FROBENIUS NORM

758
759
760
761

Norm-based metrics were originally shown to be too coarse a metric to measure the generalisability of the neural networks in Zhang et al. (2022). Figure 7 strengthens these findings, highlighting that there is essentially no correlation between the Frobenius Norm of a layer and the test accuracy of a model.

762



796

797

Figure 7: Layer re-initialisation (blue) and re-randomisation (orange) test accuracy vs Frobenius Norm. ρ is the Spearman correlation coefficient, $RMSE$ is the root mean square error of the linear regression (red line), and $K-\tau$ is the Kendall's tau measure, all with respect to the relationship between test accuracy and alpha values.

802

803

804

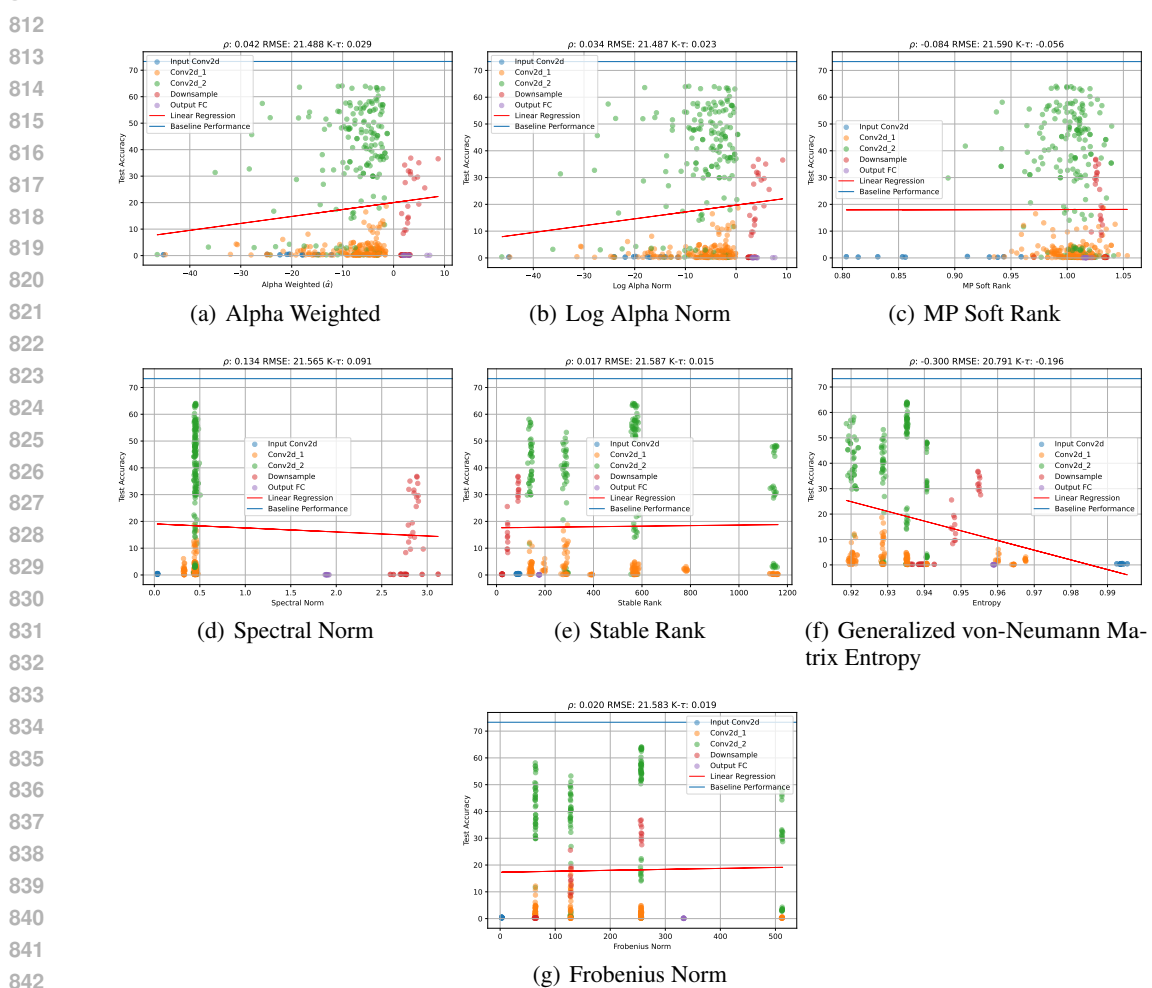
805

806

807

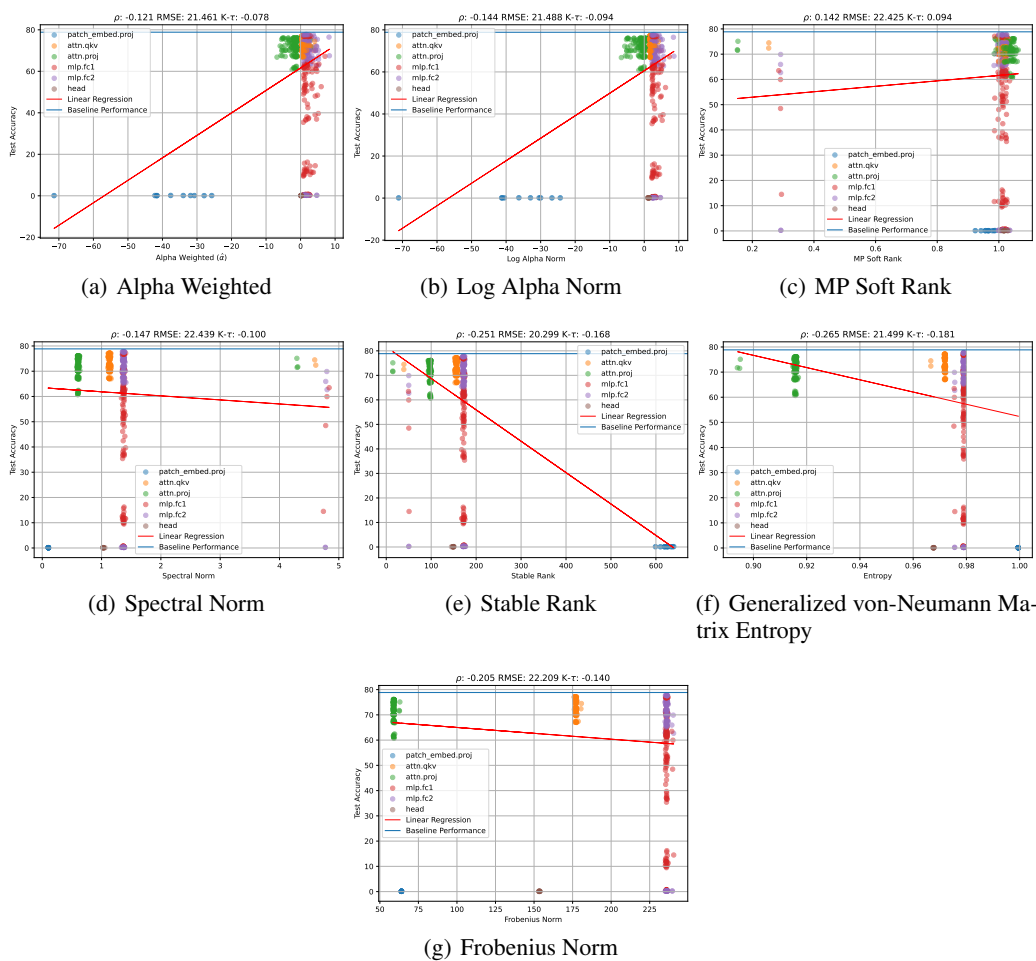
808

809

810 A.2 RESNET34 ON IMAGENET
811

844 Figure 8: ResNet 34: Layer re-randomisation test accuracy vs the respective metric. ρ is the Spearman
845 correlation coefficient, $RMSE$ is the root mean square error of the linear regression (red line), and
846 $K-\tau$ is the Kendall's tau measure, all with respect to the relationship between test accuracy and the
847 metric.

848 In Figure 8, we observe the same trend as found with α in the main body of the paper. While some
849 correlations are higher than circa 0, i.e. (f) we can clearly observe that there is strong overlap between
850 the values and the accuracy and that is induced by the different layer types explored.
851

864 A.3 ViT ON IMAGENET
865
866

898 Figure 9: ViT: Layer re-randomisation test accuracy vs the respective metric. ρ is the Spearman
899 correlation coefficient, $RMSE$ is the root mean square error of the linear regression (red line), and
900 $K-\tau$ is the Kendall's tau measure, all with respect to the relationship between test accuracy and the
901 metric.

902
903 In Figure 9, we observe the same trend as found with α in the main body of the paper. While some
904 correlations are higher than circa 0, i.e. (f) we can clearly observe that there is strong overlap between
905 the values and the accuracy and that is induced by the different layer types explored.
906
907
908
909
910
911
912
913
914
915
916
917

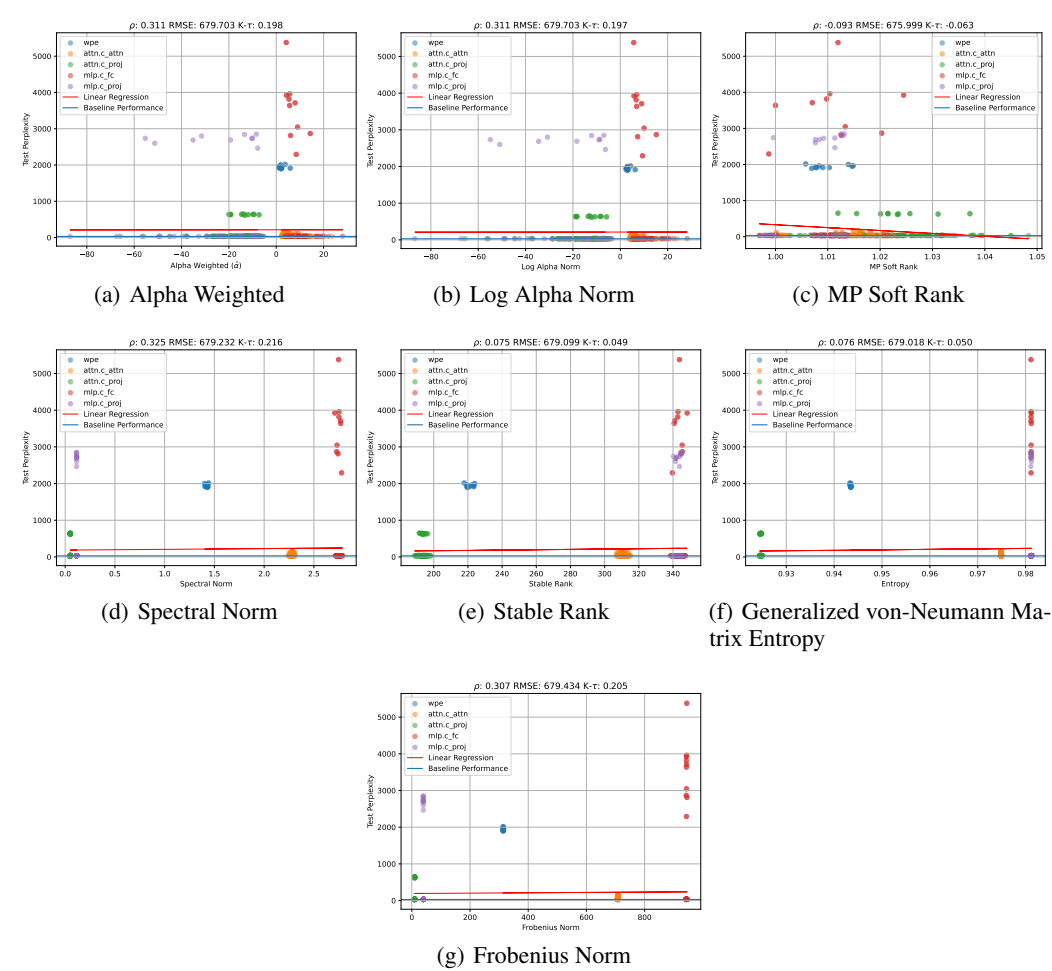
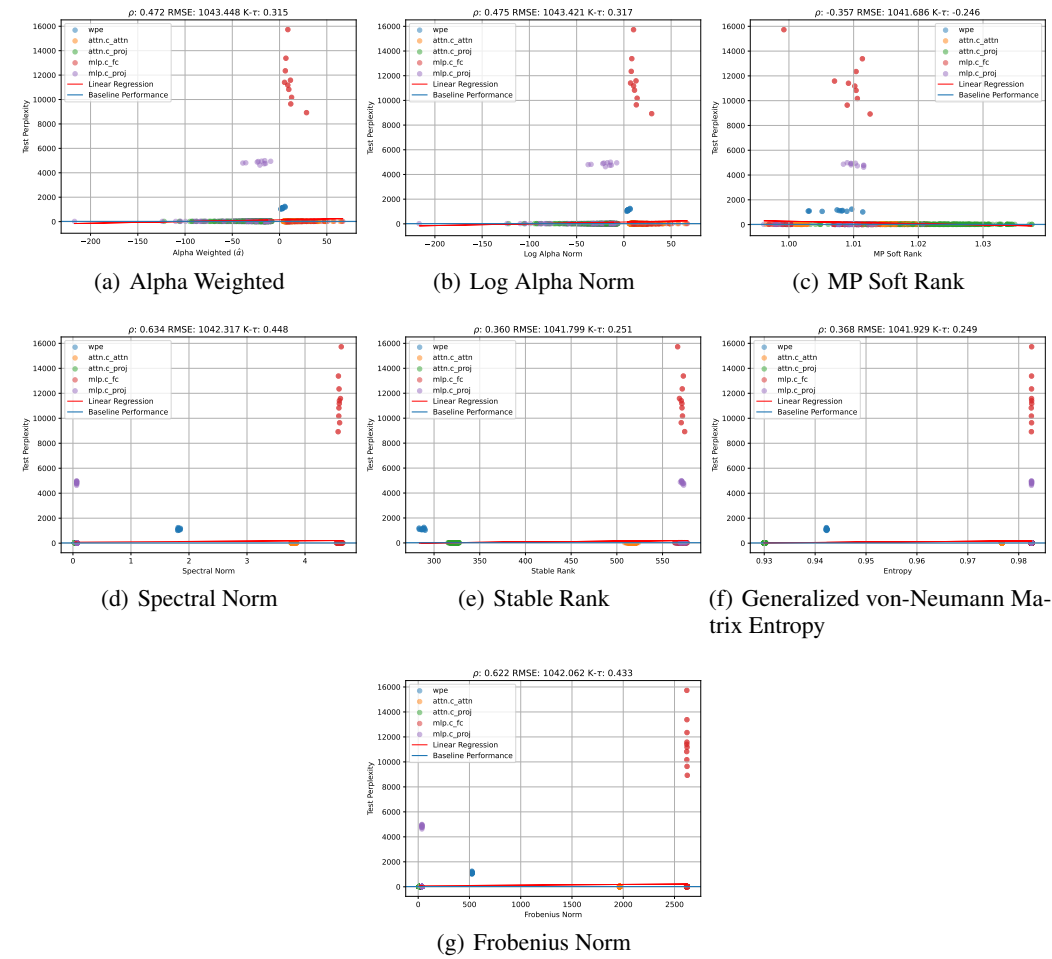
918 A.4 GPT2 ON WIKITEXT103
919

Figure 10: GPT2: Layer re-randomisation test accuracy vs the respective metric. ρ is the Spearman correlation coefficient, $RMSE$ is the root mean square error of the linear regression (red line), and $K\text{-}\tau$ is the Kendall’s tau measure, all with respect to the relationship between test accuracy and the metric.

In Figure 10, we observe the same trend as found with α in the main body of the paper, across all metrics explored.

972 A.5 GPT2-LARGE ON WIKITEXT103
973
974

1006 Figure 11: GPT2-Large: Layer re-randomisation test accuracy vs the respective metric. ρ is the
1007 Spearman correlation coefficient, $RMSE$ is the root mean square error of the linear regression (red line),
1008 and $K-\tau$ is the Kendall's tau measure, all with respect to the relationship between test accuracy
1009 and the metric.

1011 In Figure 11, we observe the same trend that there is little to no correlation between the metric and the
1012 test accuracy of the model as found with α in the main body of the paper, across all metrics explored.
1013

1014 B CONNECTION TO THE LOTTERY TICKET HYPOTHESIS
1015

1017 For our MNIST experiments, both re-initialisation and re-randomisation are drawn from the Uniform
1018 distribution, $\mathcal{U}(-\sqrt{k}, \sqrt{k})$ where k is $\frac{1}{\text{in_features}}$. However, a layer can reduce to random accuracy
1019 under re-randomisation but not under re-initialisation, which suggests that an important factor for
1020 performance retention under re-initialisation is the signs of the weights, as this represents the only
1021 difference between re-randomisation and re-initialisation.

1022 The signs of the weights, especially within networks that use the ReLU activation, essentially
1023 represent the pathway, or subnetworks within the model, which are directly related to the Lottery
1024 Ticket Hypothesis (LTH) (Frankle & Carbin, 2018). The LTH suggests that at random initialisation,
1025 there exist subnetworks that, when trained, reaches the test accuracy of the original model that is
trained with all the parameters and same compute budget (Frankle & Carbin, 2018).

To explore the role of the signs, we take the re-randomised values for a layer and apply the signs of the re-initialised layer to the re-randomised weights. We explore this using the data-based metrics that can disambiguate between re-initialised and re-randomised layers, see Figure 12. We find in Figure 12 that when applying the signs of the re-initialisation to the magnitudes of the re-randomisation layer (**green** in Figure), this layer is closer to the original layer as observed with a reduction in difference, and that there is an increase in performance when compared to the re-randomised layer (**orange** in Figure).

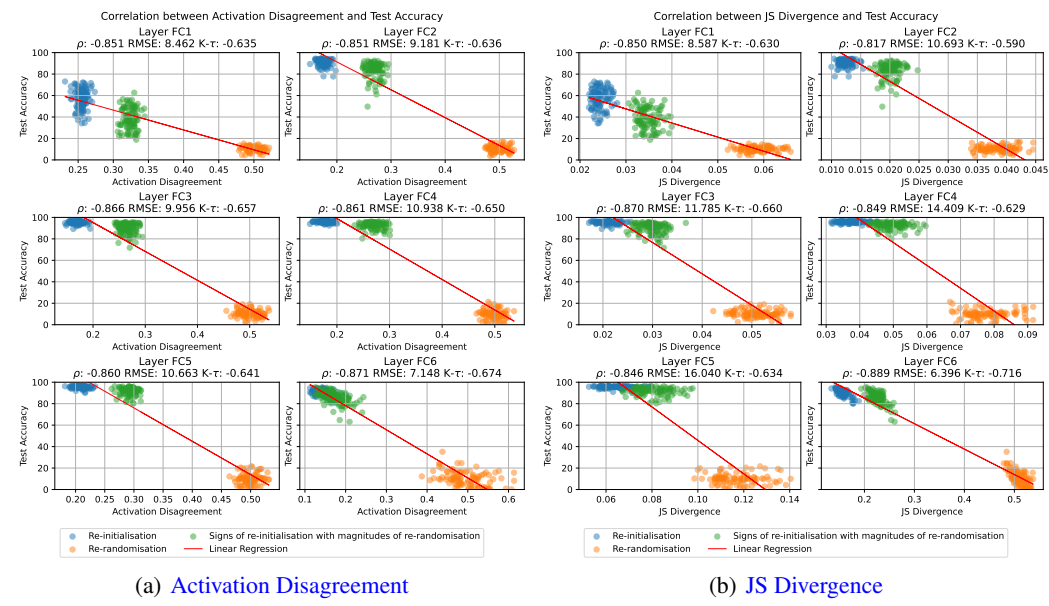


Figure 12: Layer re-initialisation (**blue**), re-randomisation (**orange**) and signs of re-initialisation with magnitudes of re-randomisation (**green**) test accuracy vs the respective metric. ρ is the Spearman correlation coefficient, $RMSE$ is the root mean square error of the linear regression (red line), and $K-\tau$ is the Kendall's tau measure, all with respect to the relationship between test accuracy and the metric.

The results strongly suggest that for this network, the subnetworks defined at the start of training through initialisation do not dramatically change through training, providing credence to the LTH. Furthermore, this demonstrates the efficacy of data-based metrics to disambiguate between the subnetwork importance of layers in neural networks, which is not captured in current data-free metrics we explore in this paper due to their inability to disambiguate robust and critical layers.

C FURTHER ANALYSIS OF DATA BASED METRICS

In this section, we additionally explore the Linear CKA metric's (Kornblith et al., 2019) power to distinguish between the output of a re-initialised layer from that of a re-randomised layer. We find that Linear CKA can disambiguate between a re-initialised and re-randomised layer. Although CKA has less predictive power than the Activation Disagreement and JS Divergence metrics explored in the body of the paper, as demonstrated with lower correlation values and higher RMSE, see Figure 13. These results show that not all data-based metrics can be considered equal and that there still remains a challenge in utilising the correct data-based metrics that effectively consider subnetwork relationships and disambiguate between robust and critical layers.

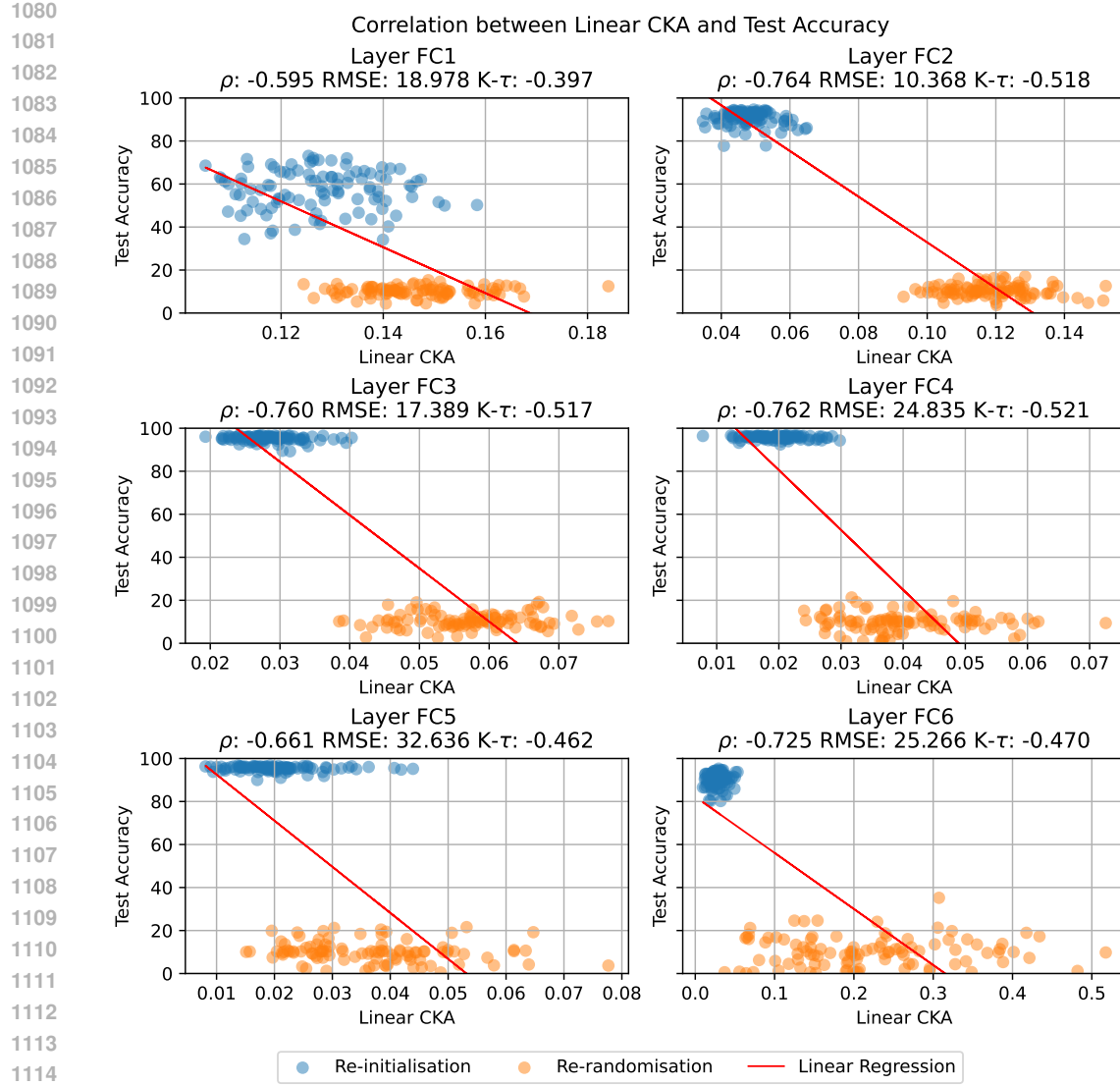


Figure 13: Layer re-initialisation (blue) and re-randomisation (orange) test accuracy vs the respective metric. ρ is the Spearman correlation coefficient, $RMSE$ is the root mean square error of the linear regression (red line), and $K-\tau$ is the Kendall's tau measure, all with respect to the relationship between test accuracy and the metric.

D LACK CAUSALITY OF ALPHA FOR GENERALISATION

We conduct the following experiments to highlight that the alpha (α) metric is not causally related to generalisation.

Firstly, we show that a model can be initialised with all layers within the so-called good range ($2 \leq \alpha \leq 6$) and achieve random performance. Also we show that having all layers initialised outside of the the so-called good range ($\alpha > 6$) achieves random performance, as presented in Section D.1. Second, we show that a model can be trained with a fixed α values within the good range ($2 \leq \alpha \leq 6$), and outside of this range ($\alpha > 6$) taht achieve comparable performance. This insight which demonstrates that the α metric is not causally related to generalisation but is a quirk of current optimisation processes, see Section D.2.

1134
1135

D.1 ALPHA AT INITIALISATION

1136
1137
1138

We explore the role of alpha at initialisation. Figure 2 shows that a layer can be randomly initialised within the so-called good range of α ($2 \leq \alpha \leq 6$). However, an α within this range is meant to indicate a well-trained layer.

1139
1140
1141
1142
1143
1144
1145
1146

Therefore, we explore the effect of initialising all layers with α within the good range ($2 \leq \alpha \leq 6$). If α is indicative of generalisation and a well-trained layer, then it can be expected that a model with all layers within the so-called good range should only achieve good generalisation and high test accuracy. To explore this question, we randomly sample initialisations such that we initialise a network where all the layers α values are within the so-called good range ($2 \leq \alpha \leq 6$) and record the test performance, we also do this for when all the layers are outside the so-called good range $\alpha > 6$ for $10 \leq \alpha \leq 12$ and $18 \leq \alpha \leq 20$ and record the test performance for a model with and without biases, see Table 4 and 5 respectively.

1147

Table 4: MLP with biases test accuracy on MNIST with layers initialised at specific α values. Mean and standard error from the mean (Belia et al., 2005) derived from 100 models.

1150

Fix Alpha Range	FC1	FC2	FC3	FC4	FC5	FC6	Test Accuracy
$2 \leq \alpha \leq 6$	5.2452 ± 0.0544	5.2002 ± 0.0555	5.0457 ± 0.0636	5.1697 ± 0.0542	5.114 ± 0.0668	5.5775 ± 0.0318	9.9374 ± 0.041
$10 \leq \alpha \leq 12$	10.8982 ± 0.0544	10.936 ± 0.0527	10.9273 ± 0.0522	10.8935 ± 0.0535	10.9935 ± 0.0574	10.9172 ± 0.0571	9.9474 ± 0.0857
$18 \leq \alpha \leq 20$	19.0811 ± 0.0519	18.8586 ± 0.0556	18.9057 ± 0.0551	19.0434 ± 0.0542	18.9315 ± 0.0552	18.9897 ± 0.0549	9.9997 ± 0.0615

1153

1154

1155
1156
1157

Table 5: MLP without biases test accuracy on MNIST with layers initialised at specific α values. Mean and standard error from the mean (Belia et al., 2005) derived from 100 models.

1158

Fix Alpha Range	FC1	FC2	FC3	FC4	FC5	FC6	Test Accuracy
$2 \leq \alpha \leq 6$	5.2452 ± 0.0544	5.2002 ± 0.0555	5.0457 ± 0.0636	5.1697 ± 0.0542	5.114 ± 0.0668	5.5775 ± 0.0318	10.0062 ± 0.165
$10 \leq \alpha \leq 12$	10.8982 ± 0.0544	10.936 ± 0.0527	10.9273 ± 0.0522	10.8935 ± 0.0535	10.9935 ± 0.0574	10.9172 ± 0.0571	10.2795 ± 0.2019
$18 \leq \alpha \leq 20$	19.0811 ± 0.0519	18.8586 ± 0.0556	18.9057 ± 0.0551	19.0434 ± 0.0542	18.9315 ± 0.0552	18.9897 ± 0.0549	9.7291 ± 0.1655

1161

1162

Table 4 and 5 show that a model can be initialised with all layers within or outside of the so-called good alpha range achieve similar accuracy (random accuracy) regardless of α . Thereby showing α has no predictive power of a model’s performance and is not casually related to generalisation.

1163

1164

D.2 TRAINING WITH ANY ALPHA

1165

1166

Within WeightWatcher⁶, for linear layers, the α metric is calculated using the squared singular values, Σ^2 , of the weight matrix. Given that random initialisations can achieve a range of α values, including those within the so-called good range ($2 \leq \alpha \leq 6$), we sample from the random initialisation for each layer to obtain singular values that correspond to a desired α value, Σ^α .

1167

1168

We then use an initialised network and decompose the layers using singular value decomposition, to obtain matrices $U\Sigma V^T$, we replace Σ with the singular values of the desired alpha, Σ^α . To obtain a new matrix, $U\Sigma^\alpha V^T$, which has the desired metric, we then keep Σ^α fixed during training, aka frozen. We then solely train U and V^T while maintaining the unitary properties of U and V^T . This ensures that the model can learn, but the alpha values minimally change through training.

1169

1170

We explore maintaining alpha values between $2 \leq \alpha \leq 6$, $10 \leq \alpha \leq 12$, and $18 \leq \alpha \leq 20$ for all layers using the same original initialisation and only replace the singular values and show the results across 10 runs on MNIST, in Table 6 and Figure 14.

1171

1172

1173

Table 6: Resulting test performance of models trained with fixed Alpha (α) values. Mean and standard error of the mean (Belia et al., 2005) derived from 10 trained models trained on MNIST.

1174

1175

1176

1177

Fix Alpha Range	FC1	FC2	FC3	FC4	FC5	FC6	Test Accuracy
$2 \leq \alpha \leq 6$	5.4799 ± 0.1312	5.0627 ± 0.1209	5.1361 ± 0.1836	4.9623 ± 0.1957	5.209 ± 0.194	5.4213 ± 0.1224	90.178 ± 0.0214
$10 \leq \alpha \leq 12$	10.7025 ± 0.1442	11.0621 ± 0.2103	10.8441 ± 0.1443	10.8218 ± 0.1284	11.0165 ± 0.138	11.2001 ± 0.2024	90.223 ± 0.0237
$18 \leq \alpha \leq 20$	19.0752 ± 0.1244	17.4638 ± 1.2448	18.8759 ± 0.1885	18.7325 ± 0.1573	18.6775 ± 0.2023	18.8356 ± 0.1289	90.219 ± 0.0253

1178

⁶<https://github.com/CalculatedContent/WeightWatcher>

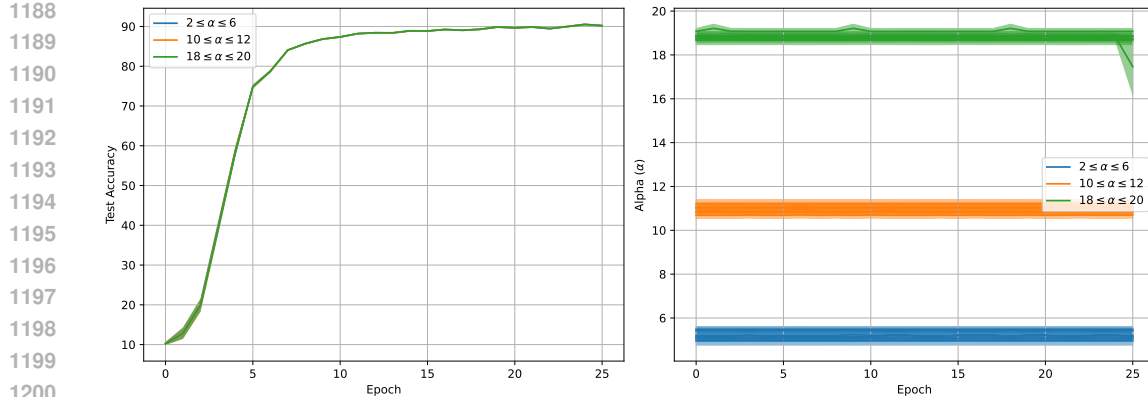


Figure 14: Test Accuracy through training with fixed α on MNIST (Left). α value of layers thought training (Right). Mean and standard error of the mean (Belia et al., 2005) (hue) derived from 10 trained models trained on MNIST.

These results in Table 6 and Figure 14 show that the model can learn and achieve good performance regardless of the fixed α .

All models, regardless of fixed α , achieve similar performance. Therefore, α between 2 and 6 is not causally related or required for good performance. It should be noted that the model does not achieve the same performance as the main body of the paper; however, this can be attributed to fixed Σ^α , which has caused a strong regularisation effect.

Furthermore, this shows that just because models generally fall within good alpha values during training, this is not a prerequisite of generalisation and more of a quirk of the current optimisation process afforded by SGD and similar variants.